ACS Sustainable Chemistry & Engineering

Research Article

Cite This: ACS Sustainable Chem. Eng. XXXX, XXX, XXX−XXX

pubs.acs.org/journal/ascecg

Metal-Free Aqueous Flow Battery with Novel Ultrafiltered Lignin as Electrolyte

Alolika Mukhopadhyay,[†] Jonathan Hamel,[†] Rui Katahira,[‡] and Hongli Zhu*[,†]

[†]Department of Mechanical and Industrial Engineering, Northeastern University, 360 Huntington Avenue, 334 Snell Engineering, Boston, Massachusetts 02115, United States

[‡]National Renewable Energy Laboratory, Denver West Parkway, Golden, Colorado 80401, United States

Supporting Information

ABSTRACT: As the number of generation sources from intermittent renewable technologies on the electric grid increases, the need for large-scale energy storage devices is becoming essential to ensure grid stability. Flow batteries offer numerous advantages over conventional sealed batteries for grid storage. In this work, for the first time, we investigated lignin, the second most abundant wood derived biopolymer, as an anolyte for the aqueous flow battery. Lignosulfonate, a water-soluble derivative of lignin, is environmentally benign, low cost and abundant as it is obtained from the byproduct of paper and biofuel manufacturing. The lignosulfonate utilizes the redox chemistry of quinone to store energy and undergoes a reversible redox reaction. Here, we paired lignosulfonate with Br_2/Br^-, and the full cell runs efficiently with high power density. Also, the large and complex molecular structure of lignin considerably reduces the electrolytic crossover, which ensures very high capacity retention. The flowcell was able to achieve current densities of up to 20 mA/cm^2 and charge polarization resistance of 15 ohm cm^2. This technology presents a unique opportunity for a low-cost, metal-free flow battery capable of large-scale sustainable energy storage.

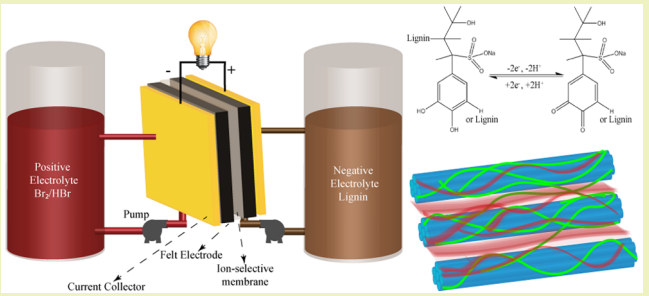

KEYWORDS: *Flow battery, Lignin, Sustainability, Abundance, Organic electrolyte, Redox active polymer*

INTRODUCTION

The need to reduce dependence on carbon-emitting forms of electricity generation has led to a recent increase in the integration of environmentally friendly energy sources.[1] Two of the most rapidly growing forms of renewable energies, solar and wind, present demand−response issues for electrical infrastructure due to their intermittent nature.[2] During high demand periods, these intermittent sources require supplemental power output in the form of either peaking power plants or electrical energy storage. Static batteries have been deployed for short duration load deferment; however, since power and energy cannot be scaled independently from one another in these batteries, they cannot be cost-effectively designed to sustain their rated power for long enough durations to efficiently defer wind and solar.[3]

Redox flow batteries do not suffer from this limitation and are therefore provide a viable path for long duration grid scale load deferment.[1] However, redox flow battery development has historically been burdened by the high costs of their materials of construction, electrolytes, and precious metal catalysts required to drive the desired redox reaction.[4] Recently, lignosulfonate has been investigated as a low cost, earth abundant material that is redox active due to its naturally forming phenol groups.[5,6] Lignin is an abundant biopolymer, comprising approximately 20−30% of the biomass of most types of wood.[6−8] Lignosulfonate is produced as a byproduct of the sulfite pulping process during paper manufacturing, and due to limited exploration of lignin derivatives for industrial application, they are often burned at a low heating value to recover their waste energy for the paper manufacturing process.[8,9] Because of the abundance of lignin, an estimated 9.8×10^5 tons per year,[10] and its limited use, lignin is an extremely low-cost material. During pulping processes for paper manufacturing, the useful pulp is extracted and separated from the rest of the material in the feedstock, leaving behind a waste product known as black liquor. This black liquor contains high concentrations of lignin, up to approximately 43 wt %[11] depending on the feedstock and pulp extraction method used. Useful lignins can easily be extracted from black liquor, and since it is a waste product of a common process, lignin is produced at very low cost but large scale and environmentally friendly. In 2013, Arkell et al. determined that ultrafiltered lignin could be produced at a concentration of 230 g L^{-1} for as little as $180 per ton.[12]

The redox functions of lignin are used in energy conversion processes in plants.[6] Because of this redox activity, lignin has been studied as a redox active species in solid pseudocapacitors. Lignin has also been used as a doping agent with polypyrroles

Received: January 15, 2018
Revised: February 25, 2018
Published: March 6, 2018

DOI: 10.1021/acssuschemeng.8b00221
ACS Sustainable Chem. Eng. XXXX, XXX, XXX−XXX

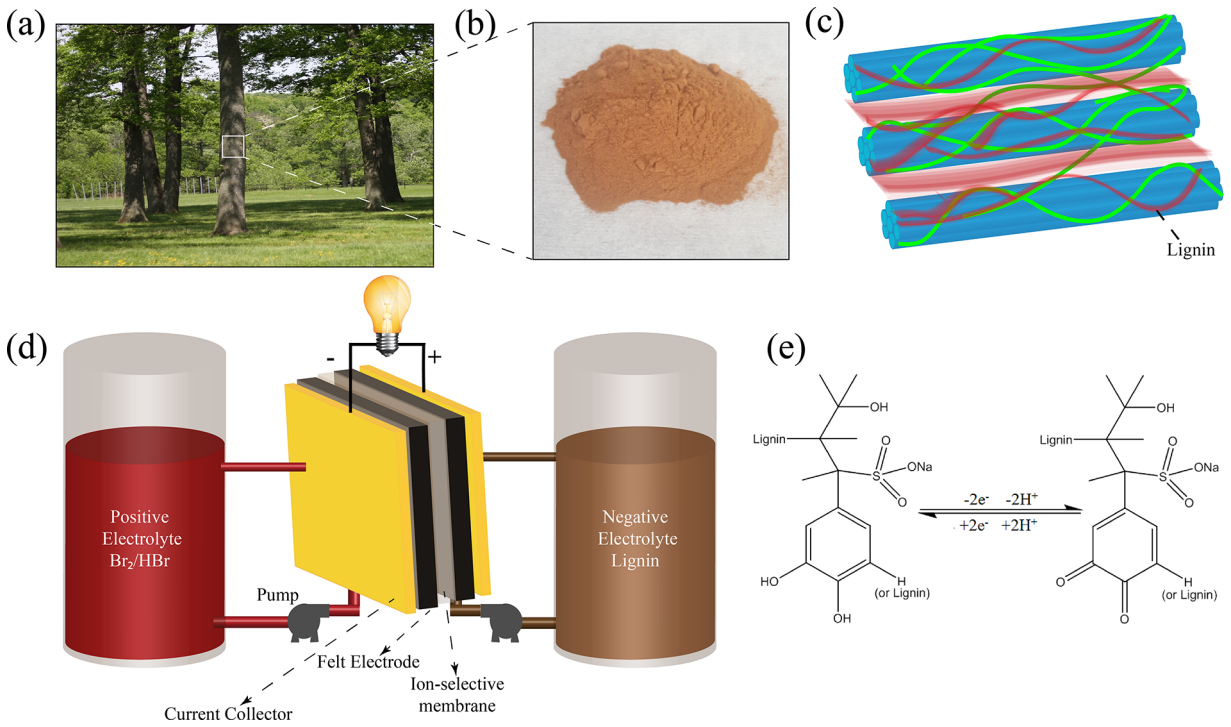

Figure 1. (a) Demonstrating the lignin in the plant. (b) Picture of lignin powder derived from black liquor, a waste product of pulping processes used in the manufacture of paper. (c) Schematic diagram of lignin distribution showing cellulose fibrils (blue) laminated with hemicellulose (green) and lignin (red) polymers. (d) Schematic of the lignin flow battery system assembly. (e) Skeletal formula of a phenol end of a lignin molecule going through a redox reaction, releasing two electrons and two protons in the process.

to make electrodes and was shown to increase the stability and conductivity of the polymer, while also improving the charge storage capacity.[5] However, until now lignin has not been used as an active species in an aqueous flow battery electrolyte. Herein, for the first time, we investigate the use of lignin as an electrolyte in a redox flow battery. Unlike many legacy flow battery technologies, lignin is sustainable, renewable, and earth-abundant, as it is a naturally occurring biopolymer. It is nontoxic to animals, does not contains any heavy metals, and is environmentally friendly. Some lignins have even been approved for use as a dust control dispersant on dirt roads, which speaks to the lack of adverse effects that lignin has on the environment. Unlike many legacy redox flow battery chemistries, lignin flow batteries could potentially be deployed at energy capacities large enough for grid-scale load deferment without posing any significant health or environmental hazards to their surroundings. This work dissolves ultrafiltered lignosulfonates in aqueous solution with a pure carbon felt with no expensive precious metal catalyst as electrode. Electrochemical characterization of the lignin solution shows a sharp oxidation peak at 0.6 V, and an obvious reduction peak at 0.45 V vs Ag/AgCl. The redox behavior of the lignin is shown to be stable and repeatable, with good capacity retention and the potential for high energy densities.

RESULTS AND DISCUSSION

Figure 1a–c shows a simplified schematic of lignin extracted from common, abundant biomass. After the pulp is removed, the lignin-rich black liquor waste product is most often dried and sent back to the plant to recover the energy from this material in the form of heat. The black liquor does not have a high heating value compared to more common forms of carbon-based heating fuel; therefore, lignin is not regarded as a useful fuel. Rather than being burned, the lignin material can easily be separated from the black liquor constituents.[13] When these methods are used on the black liquor byproduct of the sulfite wood pulping process, sulfonated lignin is produced and can be dried to yield a fine brown powder, which is shown in Figure 1b. These sulfonated lignins also called lignosulfonates, are highly water-soluble and can be easily dissolved in many acids. Lignins are coupled with cellulose and hemicellulose with hydrogen bond and chemical bonds, as shown inFigure 1c. In this study, in order to get relatively higher phenol content in the lignin, we used ultrafiltered lignin, which is treated Figure 1d, consists of two aqueous electrolytes separated by an ion exchange membrane. Solutions of lignosulfonate in perchloric acid (negative electrolyte) and hydrobromic acid in bromine (positive electrolyte) were pumped through the flow cell chambers. The Br_2/HBr electrolyte was chosen as a counterpart to study the lignin electrolyte because of its high standard reduction potential and well-understood redox properties. Each electrolyte chamber held soft carbon felt electrodes with no catalysts, which were compressed against graphite nonopolar plates with a column flow pattern machined in them to form the electrolyte chamber. The entire assembly was compressed by gold plated copper current collectors, which were connected to a potentiostat for electric power and load.

Lignosulfonates contain naturally occurring phenol groups, which undergo a reversible two-electron, two-proton charge transfer when dissolved in a suitable charge carrying electrolyte and put under elevated electric potential on the carbon electrode. Figure 1e illustrates a fraction of the lignin molecule undergoing this phenol/quinone reaction, releasing two electrons and two protons in the process. The lignin molecule is much larger than what is shown in the figure, and the exact chemical structure of lignin is complex.[14,15] The phenol groups

DOI: 10.1021/acssuschemeng.8b00221
ACS Sustainable Chem. Eng. XXXX, XXX, XXX−XXX

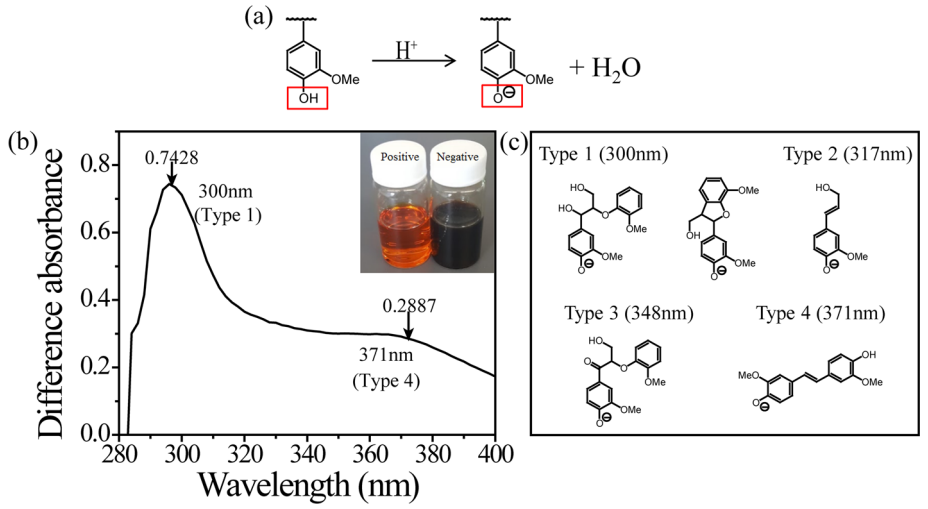

Figure 2. (a) Ionization reaction of lignin. Under basic condition, phenolic−OH of lignin is ionized to O^-. (b) Ionization difference UV spectrum of ultrafiltered lignin and the inset shows the digital image of positive and negative electrolyte pair. The arrows point at the two ΔD_{max} of ionization differences in the UV spectrum of ultrafiltered lignin at ∼0.74 at 300 (type 1) and ∼0.29 at 371 nm (type 4). (c) Structural details and the absorbance wavelength of four different groups present in lignin.

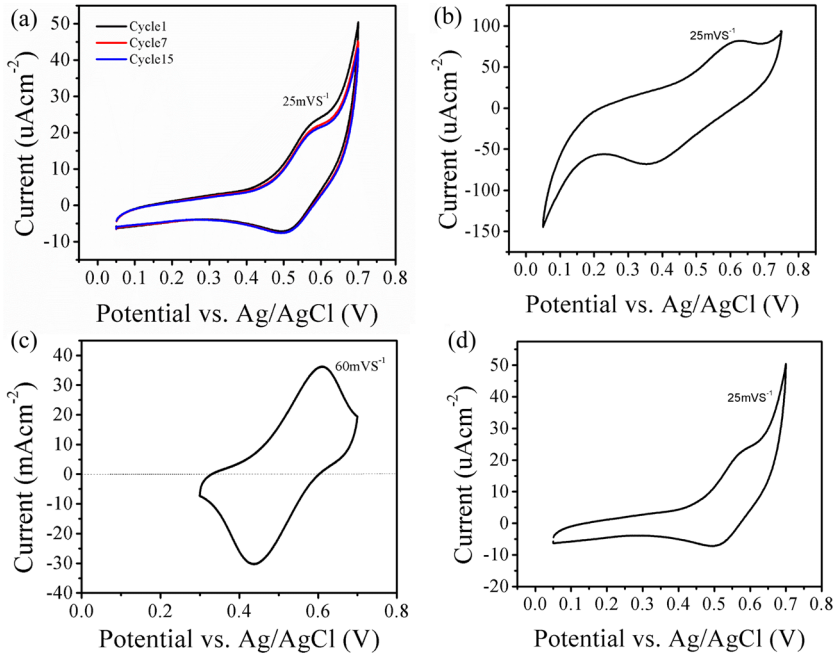

Figure 3. CV scans of ultrafiltered lignin material with (a) multiple cycles on a gold working electrode, (b) diluted electrolyte on a glassy carbon working electrode, (c) dried active material on a carbon paper working electrode. (d) Commercially available lignin on a glassy carbon working electrode.

are the part of the lignin molecule that participate in the redox reaction, and the rest of the molecule shows no signs of degradation even under repeated redox cycling.

The physical properties of various candidate lignins were studied to determine the best electrolyte formulation to use in the lignin flow battery. The organic structure, molecular weight, and phenol content of lignosulfonate vary widely depending on the feedstock from which it was extracted, the extraction process used, and the methods of filtration and drying.[16] Size exclusion chromatography (SEC) was performed on the lignosulfonate sample that performed best in the flow battery and yielded a molecular weight of 4000, which is on the lower end of the molecular weight range for biopolymer lignins.[17]

The Figure 2a shows that under basic conditions, phenolic of lignin is ionized to quinone leading to to a shift in UV spectrum. The ionization difference UV spectrum of ultrafiltered lignin has two ΔD_{max} of 0.7428 at 300 nm (type 1) and 0.2887 at 371 nm (type 4) as shown in Figure 2b,c. Therefore, the phenol content of ultrafiltered lignin was determined using ionization difference UV spectrum which showed a result of 1.54 wt %. Another analysis of functional groups was performed in our previous work[18] through quantitative P NMR analysis, showing an average phenol group concentration of 1.11 mmol g^{-1} for this material. This combination of high phenol concentration and low molecular weight is critical to the success of the battery. In addition, the large size of lignin

DOI: 10.1021/acssuschemeng.8b00221
ACS Sustainable Chem. Eng. XXXX, XXX, XXX−XXX

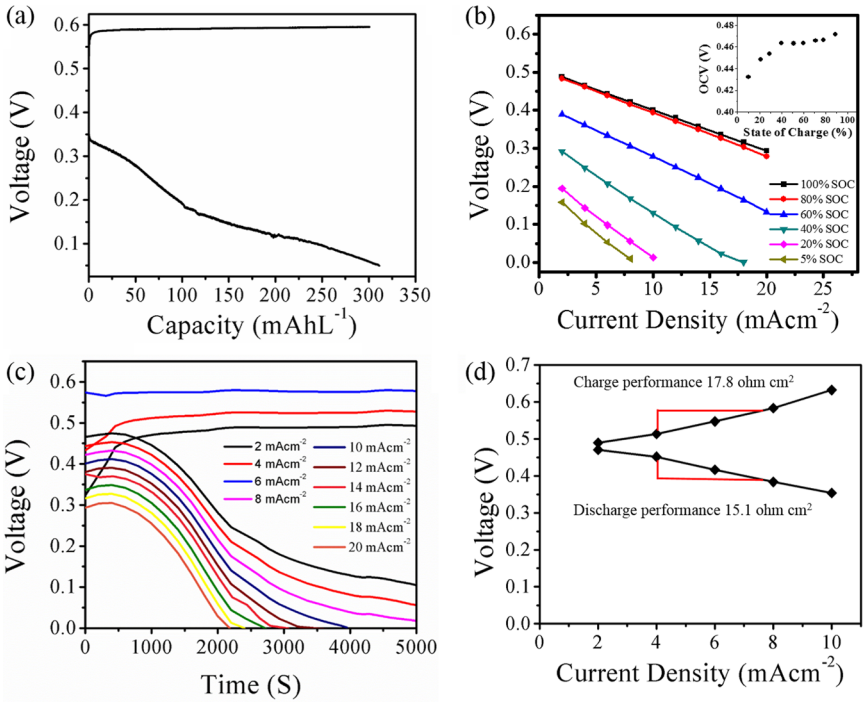

Figure 4. (a) Voltage traces during galvanostatic charge and discharge at 10 mA cm^{-2}. (b) OCV at various states of charge. (c) Cell voltage vs time at various current densities. (d) Polarization curve during charge and discharge at various current densities.

molecule compared to those of traditional metal-based electrolytes will also reduce the amount of crossover of lignin to the positive electrolyte, which will further increase the stability of the cell. The high phenol concentration ensures the presence of active materials to facilitate the redox reaction even at modest electrolyte flow rates, while the low molecular weight ensures that the viscosity of the electrolyte solution stays in a range, as shown in Figure S1, where the material can move freely through the flow field without using excess pump power or risking damage to the ion exchange membrane. Therefore, a solution of 0.1 M lignin dissolved in 0.1 M perchloric acid was formulated as the negative electrolyte, with an approximate energy capacity of 7 Wh L^{-1} when used with Br_2/HBr as a redox couple. The pH of the negative electrolyte was ~1. Higher concentrations with higher energy densities can easily be made as the solubility of lignosulfonate is ~0.2 ML^{-1} in water and mild acids,[19] and the higher concentration solution can be used when the cell is better engineered. However, for this proof of concept the concentration was intentionally kept low in order to facilitate flow through the battery chamber. The 0.1 M lignosulfonate is highly soluble in perchloric acid and forms a dark brown solution with a viscosity of 0.05 Pa·s at 25 °C (Figure 2b, inset). During the initial testing the lignin/bromine battery showed signs of the proper redox reactions occurring and the system operating correctly.

To gain further insight into the redox reaction in the lignin phenol groups, half-cell measurements were performed on the lignosulfonate material. Figure 3a–c show cyclic voltammetry of the lignosulfonate material in 0.1 M perchloric acid with various working electrodes. All show a single step electron transfer with high symmetry centering at 0.50 V vs Ag/AgCl. This is consistent with the open circuit voltage against Br_2/HBr in the flow battery (opposing half reaction: $Br_2 + 2e^- \leftrightarrow 2Br^-$ 0.89 V vs Ag/AgCl).[20] The symmetry and apparent redox reversibility are attributed to the stability of the oxidized lignin product in acidic conditions.

Figure 3a,b were tested at a scan rate of 25 mV s^{-1} with the lignin material in solution at a concentration of 0.3 mML^{-1}. Both of these show ends which are not second peaks but are inherent from the background trace of the supporting perchloric acid electrolyte. Due to the limited amount of phenol groups available in such a dilute solution, the reduction and oxidation peaks are not very large but still clearly show reversible redox behavior. Figure 3a shows a trace of the lignin material being cycled 15 times on a gold foil working electrode without any substantial indications of irreversibility, aside from the first cycle. This reduction in peak size after the first cycle was observed consistently over a number of trials and is likely due to dissolved oxygen in the solution oxidizing the lignosulfonate before it is depleted. This irreversibility is not observed in the flow battery, where the experimental setup allowed easy removal of dissolved oxygen prior to battery operation. Figure 3b shows a single cycle on a glassy carbon working electrode. Again, the reversibility of the peaks is apparent, and the peaks are not too large in part due to the low concentration of lignin used in these tests. The higher separation of peaks on the glassy carbon electrode compared to the gold foil electrode indicate more polarization of the electrode, which in turn implies a slower reaction kinetic.[21] Still, the peak separations of these cyclic voltammogram (CV)'s are all approximately 100 mV, which is larger than the $59/n$ mV = 29.5 mV (with n = 2 being the number of electrons involved in the redox process) expected for this reaction. This implies that equilibrium is not being established rapidly at the surface of the electrode.[4] The effects of this slow equilibrium behavior are also apparent in the full cell flow battery testing.

In an attempt to simulate the half-cell behavior of higher concentration lignin in the flow battery without the penalty of high resistance from the electrodes being separated in the CV

DOI: 10.1021/acssuschemeng.8b00221
ACS Sustainable Chem. Eng. XXXX, XXX, XXX−XXX

setup, another set of CV's was performed using lignin that was deposited and dried on a carbon paper working electrode. Results from this test at a scan rate of 60 mV s^{-1} are shown in Figure 3c, with much larger peaks than the half-cell testing in solution, as well as slightly faster reaction kinetics. A background trace of the 0.1 M perchloric acid is shown by the dotted line. Figure 3d is a CV of a different lignosulfonate material that was commercially obtained from TCI America, scanned at 25 mV s^{-1} on a gold foil working electrode. This lignin shows a second, larger set of peaks centering around 0.2 V. The smaller peaks centered around 0.5 V that were present in the other lignin can also be seen in the TCI lignin trace. The redox peaks at lower voltage created a larger open-circuit voltage (OCV) for the battery, which is beneficial to the battery performance and appear to be more active than the peaks centering around 0.5 V. However, this particular lignin did not show cyclic performance that was as strong as the other material, and thus was not included in the following flow battery test. Still, the promising half-cell behavior of this type of lignin shows that the electrochemical activity of lignosulfonates can vary depending on the feedstock and extraction methods. Other lignins such as the TCI America lignosulfonate may be interesting to study further in future work.

Voltage traces of the lignin battery at a current density of 10 mA cm^{-2} are shown in Figure 4a. The charge curve is limited to the amount of coulombs that were discharged, and because the positive side of the battery was not configured to be capacity limiting, the voltage remains on the plateau throughout the entire charge and does not increase rapidly prior to being cut off. More interesting is the discharge curve, which shows a clear plateau at 150 mV in agreement with the half-cell measurements and shows a more rapid voltage decrease as the lignin runs out of phenol groups that have not yet been oxidized. During this charge/discharge process, the OCV of the battery increased, almost linearly, from 0.43 to 0.47 V (Figure 4b). In the inset of Figure 4b, the cell voltage is plotted against current density at various states of charge (SOC). The power density of the battery shows a significant decrease at lower states of charge, specifically below 60%. This further confirms that limitations in the reactants mass transport have a significant impact on the cell voltage.[3] The ends of the best fit lines for each SOC diverge as current density increases, as expected with mass transport limitations. Voltage traces for galvanostatic charging and discharging at various current densities are shown in Figure 4c. The voltage efficiency was as high as 94% at a low current density (2 mA cm^{-2}) and did drop appreciably as current density increased. The low overall efficiency beyond current densities of 10 mA cm^{-2} is indicative of negative mass transport effects at high current densities.[22] The relatively low OCV of the battery system is also a contributing factor to the rapid drop in voltage efficiency. The electrodes of the cell were plasma treated[23] to reduce the polarization resistance by increasing the wettability between electrode and electrolyte as shown in Figure S2. The polarization curves of this configuration show that it was able to achieve low cell resistances (Figure 4d) as low as 15.1 ohm cm^2 on charge and 17.8 ohm cm^2 on discharge with good repeatability.

CONCLUSION

A lignin-based flow battery electrolyte was developed for the first time, meeting the energy storage industry demands of low cost, sustainability, and low toxicity. An array of candidate electrolytes was synthesized using lignosulfonate as the primary active material, and electrochemical testing was performed on these electrolytes to fine-tune them for optimal performance and durability in a flow battery system. The lignosulfonate material showed reversible redox peaks capable of going through multiple reduction/oxidation cycles without any appreciable decrease in activity. The battery was able to reach current densities of up to 20 mA cm^{-2} and polarization resistance as low as 15.1 ohm cm^2 as well as achieving voltage efficiencies as high as 85% at low current density. This approach of using a naturally occurring active material is vastly different from existing flow battery technologies, which mostly rely on expensive materials. This study represents an inexpensive and promising path for distributed scale energy storage.

EXPERIMENTAL SECTION

Electrolyte Preparation. First, 200 mL of 0.5 M bromine solution and 0.25 M hydrobromic acid in DI water were used in the fully charged state. Both the bromine and hydrobromic acid were commercial material obtained from Sigma-Aldrich.

The negative electrolyte solution was made by heating 50 mL of DI water to 50 °C and stirring in 0.1 M of dry lignosulfonate powder. After the powder was thoroughly dissolved, the solution was spiked with enough 70% (w/w) perchloric acid (Sigma-Aldrich) to bring the acid concentration of the solution to 0.1M. The solutions were then loaded into 250 mL electrolyte tanks for use in the flow battery system.

Flow Battery Test Apparatus. The flow battery system consisted of a single battery cell assembly, two electrolyte tanks, peristaltic pumps for electrolyte circulation, temperature control equipment, and pressure monitoring equipment. The electrolyte tanks used were 250 mL glass flasks. For temperature stability, they were submerged in water and placed on a Fisher Scientific Isotemp Stirring Hot Plate (SP88857200). The negative electrolyte tank was sealed from the atmosphere and constantly purged with nitrogen to limit oxygen interaction with that electrolyte. Before entering the tank, this nitrogen was hydrated with 0.1 M perchloric acid in a liquid trap in order to prevent excessive electrolyte evaporation. The electrolyte pumps were MasterFlex L/S heads (HV-07516−02) powered by a L/S economy variable speed drive (HV-07554−80). Cell inlet pressures were monitored by analog pressure gauges with CPVC gauge guards. All interconnections were made with flexible PVC tube and barbed PVDF tube fittings. The flow battery cell was placed above the rest of the system for easy draining between tests.

Two cell assemblies were used to qualify the lignin flow battery. The first assembly was a Fuel Cell Store Flow Battery Flex Stak (FS) (3101603). This consisted of a single cell with a 10 cm^2 active area, and a machined interdigitated flow field on the solid graphite plates. Soft goods were held in place and sealed by 2 layers 1/64 in. PTFE gaskets on each side. The current collectors were copper and encased in machined PVC pressure plates. The eight machine screws along the outside of the cell were torqued to 15 in.-lbs to hold the assembly together.

The other cell used was a fuel cell store flow battery hardware (FBH) assembly (72108114), consisting of a single cell, 5 cm^2 active area. This cell had column flow patterns machined into the solid graphite plates, with separate terminals for direct voltage referencing directly on the plate. The cell was sealed by 1/16 or 1/32 in. gaskets depending on the soft goods configuration used. End plates were 1/4 in. thick, gold-plated aluminum, which also served as the current collectors. Each end plate included a 60W heater to regulate cell temperature. The assembly was held together by 8 machine screws torqued to 15 in.-lbs.

The temperature of the flow battery electrolytes was maintained at 30 °C, and the 2x 60 W heaters on the FBH cell were plugged in during tests on that assembly. Flow rates remained constant at approximately 250 mL/min. The flow fields of all cells were configured in a coflow pattern, with the inlet at the bottom of the cell and the outlet at the top in order to mitigate the potential for hydrogen gas

DOI: 10.1021/acssuschemeng.8b00221
ACS Sustainable Chem. Eng. XXXX, XXX, XXX−XXX

vapor locking. Inlet pressures were maintained below 0.5 bar gauge, and differential pressure across the membrane was maintained below 0.1 bar differential. The battery was powered by a BioLogic MPG2 16 channel potentiostat controlled with BioLogic EC-Lab data acquisition and control software.

Plasma Pretreatment. Carbon felts and carbon papers were pretreated using a Unaxis Plasma-Therm 790 system at 13.56 MHz frequency for the plasma excitation. During the oxygen plasma treatment, system pressure and oxygen flow rate were kept constant at 2 mT and 25 sccm, respectively. RF plasma power was 150 W and the exposure time was 15 s.

Membrane Pretreatment. The membrane pretreatment method involved a 24 h soak in 0.1 M perchloric acid at room temperature, followed by triple rinsing in DI water prior to loading in the cell.

Viscosity Measurement. Viscosity testing was performed on candidate solutions by a Discovery HR-2 Rheometer (TA Instrument, USA) at 25 °C. The samples were measured at a shear rate from 0.01 to 100 s^{-1}.

Ionization Difference UV Spectrum. Analysis of functional groups was performed through quantitative Ionization difference UV spectrum. The analysis was carried on according to the method described in the literature.[24,25]

Size-Exclusion Chromatography (SEC). Molecular weight distributions of the samples were investigated by dissolving 5 mg of lyophilized samples in 2 mL of DMSO+0.5% LiBr (w/w) solution. After filtration of the samples through 0.45 um PTFE filters, size exclusion chromatography was performed on an SEC 1260 Infinity instrument (Polymer Standard Services, Germany). The equipment consisted of an isocratic pump (G1310B), a micro degasser (G1379B) and a standard autosampler (G1329B). The detection system included a UV detector (G1314B) in series with a refractive index detector (G1362A). The mobile phase was DMSO+0.5% LiBr set to a constant flow rate of 0.5 mL/min for a total run time of 65 min. The injection volume was 100 μL. The separation system consisted of PSS GRAM Precolumn, PSS GRAM 100 Å, and PSS GRAM 10000 Å analytical columns thermostated at 60 °C and connected in series. The pullulan standards with nominal masses of 708, 337, 194, 47.1, 21.1, 9.6, 6.1, and 1.08 kDa and 342 Da were used for standard calibration.

pH and Conductivity Test. pH and conductivity measurements were taken using an Oakton pH/CON Portable Meter (PC 450). Calibration was done at room temperature using Oakton 1413 and 12 880 μS conductivity standards (WD-00653-18, WD-00606-10) and Oakton 4 and 7 pH buffers (EW-00654-00, EW-00654-04)

Cyclic Voltammetry. Half-cell measurements were performed on a BioLogic SP150 single-channel potentiostat controlled by BioLogic EC-Lab software. Voltage and current were logged at 0.1 mV increments. Generally the voltage was ramped between 0.1 and 0.7 V. However, some of the voltammogram traces presented in this work are trimmed for clarity and to emphasize the redox peaks. Constant scan rates of 25 and 60 mV/s were used on all of the presented data.

For CV measurements on lignin solutions, 60 mg of dried lignin powder was dissolved in 50 mL of 0.1 M perchloric acid and stirred at room temperature for 5 min. For measurements on dried lignin, solutions of 0.1 M lignin in DI water were dropped on 10 × 20 mm AvCarb carbon paper (P50) working electrodes and allowed to dry for 24 h. The working electrode with the dried lignin was then immersed in 50 mL of 0.1 M perchloric acid for CV measurements.

All CV experiments used a single-junction Fisher Scientific Accumet Glass Body Ag/AgCl Reference Electrode (1362053) with 4 mol/L KCl filling solution, and a platinum foil counter electrode. A variety of working electrodes were used, including the aforementioned carbon paper, gold foil, and a 5 mm diameter glassy carbon electrode. Prior to each use, the glassy carbon electrode was polished on 600 grit paper with polishing compound, sonicated for 10 min in methanol, followed by a 10 min sonication in DI water. The CV's were performed in a 125 mL three-necked flask and purged with argon gas unless otherwise noted.

■ ASSOCIATED CONTENT

Supporting Information

The Supporting Information is available free of charge on the ACS Publications website at DOI: 10.1021/acssuschemeng.8b00221.

Dynamic viscosities at different shear rates, contact angles, TGA data, cost estimation method (PDF)

■ AUTHOR INFORMATION

Corresponding Author

*Hongli Zhu. E-mail: h.zhu@neu.edu.

ORCID

Hongli Zhu: 0000-0003-1733-4333

Author Contributions

A.M. and J.H. contributed equally to this work.

Notes

The authors declare no competing financial interest.

■ ACKNOWLEDGMENTS

This research was financially supported by the start-up grant and Tier1 fund to H.Z. from Northeastern University. We thank Gunnar Henriksson in KTH Royal Institue for providing the ultrafiltered lignin. We also appreciate the use of the facilities at George J. Kostas Nanoscale Technology and Manufacturing Research Center at Northeastern.

■ REFERENCES

(1) Soloveichik, G. L. Flow Batteries: Current Status and Trends. *Chem. Rev.* **2015**, *115* (20), 11533.

(2) Noack, J.; Wietschel, L.; Roznyatovskaya, N.; Pinkwart, K.; Tübke, J. Techno-Economic Modeling and Analysis of Redox Flow Battery Systems. *Energies* **2016**, *9*, 627.

(3) Yang, B.; Hoober-Burkhardt, L.; Wang, F.; Surya Prakash, G. K.; Narayanan, S. R. An Inexpensive Aqueous Flow Battery for Large-Scale Electrical Energy Storage Based on Water-Soluble Organic Redox Couples. *J. Electrochem. Soc.* **2014**, *161* (9), A1371−A1380.

(4) Huskinson, B. T.; Marshak, M.; Suh, C.; Er, S.; Gerhardt, M.; Galvin, C. J.; Chen, X.; Aspuru-Guzik, A.; Gordon, R. G.; Aziz, M. J. A metal-free organic−inorganic aqueous flow battery. *Nature* **2014**, *505*, 195.

(5) Miroshnikov, M.; Divya, K. P.; Babu, G.; Meiyazhagan, A.; Reddy Arava, L. M.; Ajayan, P. M.; John, G. Power from nature: designing green battery materials from electroactive quinone derivatives and organic polymers. *J. Mater. Chem. A* **2016**, *4* (32), 12370−12386.

(6) Milczarek, G.; Inganäs, O. Renewable cathode materials from biopolymer/ conjugated polymer interpenetrating networks. *Science (Washington, DC, U. S.)* **2012**, *335* (6075), 1468.

(7) Montague, L. *Lignin Process Design Confirmation and Capital Cost Evaluation*; Report 42002/02; National Renewable Energy Laboratory: Golden, CO, 2003.

(8) Hakeem, K. R.; Jawaid, M.; Alothman, O. Y. *Agricultural Biomass Based Potential Materials*; Springer: Cham, 2015.

(9) Al-Lagtah, N. M. A.; Al-Muhtaseb, A.; Ahmad, M. N. M.; Salameh, Y. Chemical and physical characteristics of optimal synthesised activated carbons from grass-derived sulfonated lignin versus commercial activated carbons. *Microporous Mesoporous Mater.* **2016**, *225*, 504−514.

(10) Matsushita, Y.; Yasuda, S. Preparation and evaluation of lignosulfonates as a dispersant for gypsum paste from acid hydrolysis lignin. *Bioresour. Technol.* **2005**, *96* (4), 465−470.

(11) Zaman, A. A.; Fricke, A. L. Effect of pulping conditions and black liquor composition on Newtonian viscosity of high solids kraft black liquors. *Ind. Eng. Chem. Res.* **1996**, *35* (2), 590−597.

DOI: 10.1021/acssuschemeng.8b00221
ACS Sustainable Chem. Eng. XXXX, XXX, XXX−XXX

(12) Arkell, A.; Olsson, J.; Wallberg, O. Process performance in lignin separation from softwood black liquor by membrane filtration. *Chem. Eng. Res. Des.* **2014**, *92* (9), 1792−1800.
(13) Toledano, A.; García, A.; Mondragon, I.; Labidi, J. Lignin separation and fractionation by ultrafiltration. *Sep. Purif. Technol.* **2010**, *71* (1), 38−43.
(14) Banoub, J. H.; Benjelloun-Mlayah, B.; Ziarelli, F.; Joly, N.; Delmas, M. Elucidation of the complex molecular structure of wheat straw lignin polymer by atmospheric pressure photoionization quadrupole time-of-flight tandem mass spectrometry. *Rapid Commun. Mass Spectrom.* **2007**, *21* (17), 2867.
(15) Higuchi, T. Biosynthesis of Lignin. *Biosynthesis and Biodegradation of Wood Components* **1985**, 141.
(16) Fang, Z.; Smith, R. L. *Production of Biofuels and Chemicals from Lignin*; Springer: Singapore, 2016.
(17) Tolbert, A.; Akinosho, H.; Khunsupat, R.; Naskar, A. K.; Ragauskas, A. J. Characterization and analysis of the molecular weight of lignin for biorefining studies. *Biofuels, Bioprod. Biorefin.* **2014**, *8*, 836−856.
(18) Geng, X.; Zhang, Y.; Jiao, L.; Yang, L.; Hamel, J.; Giummarella, N.; Henriksson, G.; Zhang, L.; Zhu, H. Bioinspired Ultrastable Lignin Cathode via Graphene Reconfiguration for Energy Storage. *ACS Sustainable Chem. Eng.* **2017**, *5*, 3553−3561.
(19) Evstigneev, E. Factors affecting lignin solubility. *Russ. J. Appl. Chem.* **2011**, *84* (6), 1040−1045.
(20) Singh, N.; McFarland, E. W. Levelized cost of energy and sensitivity analysis for the hydrogen− bromine flow battery. *J. Power Sources* **2015**, *288*, 187−198.
(21) Oyaizu, K.; Hatemata, A.; Choi, W.; Nishide, H. Redox-active polyimide/carbon nanocomposite electrodes for reversible charge storage at negative potentials: expanding the functional horizon of polyimides. *J. Mater. Chem.* **2010**, *20* (26), 5404.
(22) Na, Z.; Xu, S.; Yin, D.; Wang, L. A cerium−lead redox flow battery system employing supporting electrolyte of methanesulfonic acid. *J. Power Sources* **2015**, *295*, 28−32.
(23) Dixon, D.; Babu, D.; Langner, J.; Bruns, M.; Pfaffmann, L.; Bhaskar, A.; Schneider, J.; Scheiba, F.; Ehrenberg, H. Effect of oxygen plasma treatment on the electrochemical performance of the rayon and polyacrylonitrile based carbon felt for the vanadium redox flow battery application. *J. Power Sources* **2016**, *332*, 240−248.
(24) Lin, S. Y. Commercial Spent Pulping Liquors. In *Methods in Lignin Chemistry*; Lin, S. Y., Dence, C. W., Eds.; Springer Berlin Heidelberg: Berlin, Heidelberg, 1992; pp 75−80.
(25) Lin, S. Y.; Dence, C. W. *Methods in Lignin Chemistry*; Springer Science & Business Media: Berlin, 2012.

DOI: 10.1021/acssuschemeng.8b00221
ACS Sustainable Chem. Eng. XXXX, XXX, XXX−XXX